Environ Earth Sci (2010) 61:187–199
DOI 10.1007/s12665-009-0335-7

ORIGINAL ARTICLE

Mineralogical and geochemical spatial analyses of a waste-rock dump at the Libiola Fe–Cu sulphide mine (Eastern Liguria, Italy)

Pietro Marescotti · Eva Azzali · Diego Servida · Cristina Carbone · Giovanni Grieco · Luisa De Capitani · Gabriella Lucchetti

Received: 15 January 2009 / Accepted: 20 October 2009 / Published online: 11 November 2009

Abstract In this work, we investigated a 3 ha sulphide-bearing waste-rock dump (Libiola Mine, Italy) using mineralogical, geochemical, and geostatistical analyses. The dumped materials were highly heterogeneous in grain size and lithology and varied both laterally and vertically. Other than the host rock of the ore, basalts and serpentinites, the dumped materials contained high amounts of low-grade chalcopyrite- and pyrite-rich mineralisations. Due to these characteristics and to the absence of minerals able to neutralise acidity, this waste-rock dump can be classified as an acid mine drainage (AMD) producer. The study confirms that AMD is still active and, in the best scenario, can persist for up to 6.17×10^3 years. The consequences of this process are of serious environmental concern as it involves strong acidification of the circulating waters, the release of potentially toxic metals into the soil, streams and rivers and the precipitation of huge quantities of secondary Fe-oxides and Fe-oxyhydroxides.

Keywords AMD · Geostatistic application · Sulphides oxidation · Waste dump · Libiola mine

Introduction

Mine waste-rock dumps are artificial landforms built up during exploitation over tens (and sometimes hundreds) of years from the accumulation of heterogeneous rocks and mineralisation fragments. They, therefore, represent complex geological systems characterised by high vertical and lateral heterogeneities in grain size, lithology, mineralogy, and chemistry. Mine waste-rock dumps originating from sulphide ore exploitation, other than the aforementioned properties, are characterised by high percentages of low-grade mineralisations and non-valuable sulphides (such as pyrite and pyrrhotite). In open-air dumps, the supergenic oxidation of the mineralised sulphide clasts triggers acid mine drainage (AMD) processes that cause the extreme acidification of the circulating waters, the release of several metals of environmental concern, and the diffuse precipitation of secondary minerals (mainly Fe-oxides, Fe-oxyhydroxides, and sulphates) within and on the top of the dumps, as well as in the surrounding streams and rivers. In abandoned sulphide mining areas, the waste-rock and tailing dumps represent the most important source of AMD and hence the most critical sites for water and soil pollution. Therefore, the knowledge of the mineralogy and chemistry of the dumped materials is necessary not only for the evaluation of the environmental impact of the abandoned sulphide mines, but also for the planning of remedial actions.

This work presents the results of mineralogical, geochemical, and geostatistical analyses undertaken in the main waste-rock dump of the Libiola Fe–Cu sulphide mine.

P. Marescotti (✉) · E. Azzali · C. Carbone · G. Lucchetti
Dipartimento per lo Studio del Territorio e delle sue Risorse (DIPTERIS), Università di Genova, C.so Europa 26, 16132 Genoa, Italy
e-mail: marescot@dipteris.unige.it

D. Servida · G. Grieco · L. De Capitani
Dipartimento di Scienze della Terra "Ardito Desio", Università di Milano, Via Botticelli 23, 20133 Milan, Italy

The study area

The Libiola mine is located 8 km behind Sestri Levante (Eastern Liguria, Italy; Fig. 1).

The sulphide ore occurs within the Jurassic ophiolites of the Northern Apennine (Vara Supergroup; Abbate et al. 1980) which consist of an ultramafic/gabbroic basement

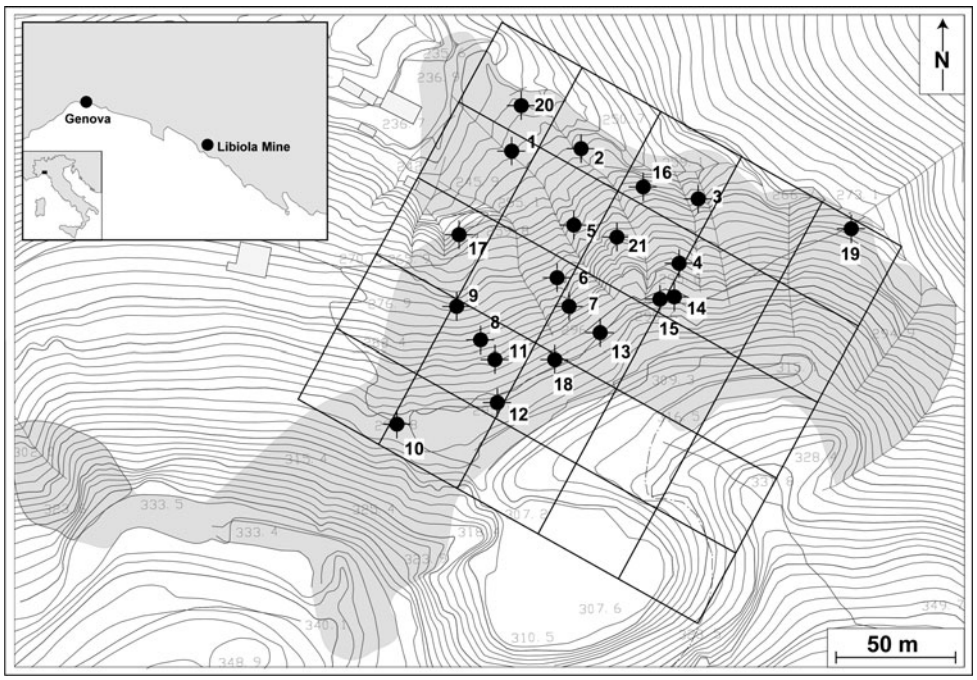

Fig. 1 Map of the waste-rock dump studied (*light grey*). The rectangular sampling area is divided into 25 square cells to form a sampling grid. The *black dots* represent the sampling points (E1–E21). In the *inset* (*top* on the *left*) is reported the geographic position of the Libiola mine

overlain by a volcano-sedimentary sequence (which in the Libiola area comprises tectonic- and sedimentary-ophiolitic breccias, pillow basalts, and cherts). This deposit has been classified as a stratabound volcanic-associated massive sulphide deposit (VMS) and occurs as massive lenses near the top of a pillow basalt sequence (Zaccarini and Garuti 2008). Non-valuable sulphide stockwork-veins, stringer ores and disseminated mineralisations are also present in the pillow basalts and serpentinised ultramafites, respectively. The sulphide mineral assemblages consist of pyrite and chalcopyrite, with minor sphalerite and pyrrhotite, in a gangue of quartz, chlorite, and minor to accessory calcite in both massive lenses and in mineralised veins. Disseminated mineralisations within the serpentinites consist almost exclusively of millimetric pyrite crystals scattered in a serpentine (lizardite and chrysotile), chlorite, and magnetite matrix.

The Libiola Fe–Cu sulphide mine was exploited from 1864 until 1962 and produced over 1 Mt of Fe–Cu sulphides with an average grade ranging from 7 to 14 wt% Cu (Marescotti and Carbone 2003; Marescotti et al. 2008). The mine covers a surface area of about 4 km^2 and comprises more than 30 km of underground tunnels (18 galleries and over 30 vertical shafts) and three major open pits.

Non-mineralised rocks (mainly basalts and serpentinites), non-valuable mineralisations (low-grade chalcopyrite and pyrite mineralisations), and tailings derived from mechanical grinding, milling, and handpicking were dumped in five main open-air waste-rock dumps and in several small bodies close to the main mine adits during the mining activities.

The climate of the Libiola mine area is Mediterranean humid and is characterised by an average temperature of 15°C. Rainfall ranges between 1,100 and 1,600 mm/year and shows a unimodal distribution with a maximum in November (180 mm) and a dry season in summer (Provincia di Genova 2002).

Waters circulating in the Libiola mine area and discharging in the adjacent streams and creeks are strongly polluted due to the diffuse occurrence of ongoing AMD processes; they are typical acid sulphate waters (ASW) being characterised by a pH as low as 2.4 and by high heavy-metal, transition-metal, and sulphate contents (Dinelli et al. 1999; Dinelli and Tateo 2002; Marini et al. 2003; Accornero et al. 2005).

The site chosen for this study is the main waste-rock dumps of the Libiola mine which is located in the northern part of the mining area. It is about 100 m in height, covers a surface of over 3 ha and has a wall slope of about 45°–50° in the upper part and of about 20°–25° in the lower part (Figs. 1, 2a).

The dump is characterised by fast, intense erosive processes (Fig. 2b) that cause several debris flows, induced by the steep wall slope and the absence of significant vegetation cover. Moreover, the northern part of the dump is adjacent to a small stream (Rio Boeno) which causes the basal erosion of its flank (Fig. 2c). The deposited materials are highly heterogeneous in grain size and in lithology and change both laterally and vertically, where centimetric to metric layering is marked by colour variations and selective erosion (Fig. 2d). Centimetric to decimetric ochreous to reddish oxidised rinds are typically present on the

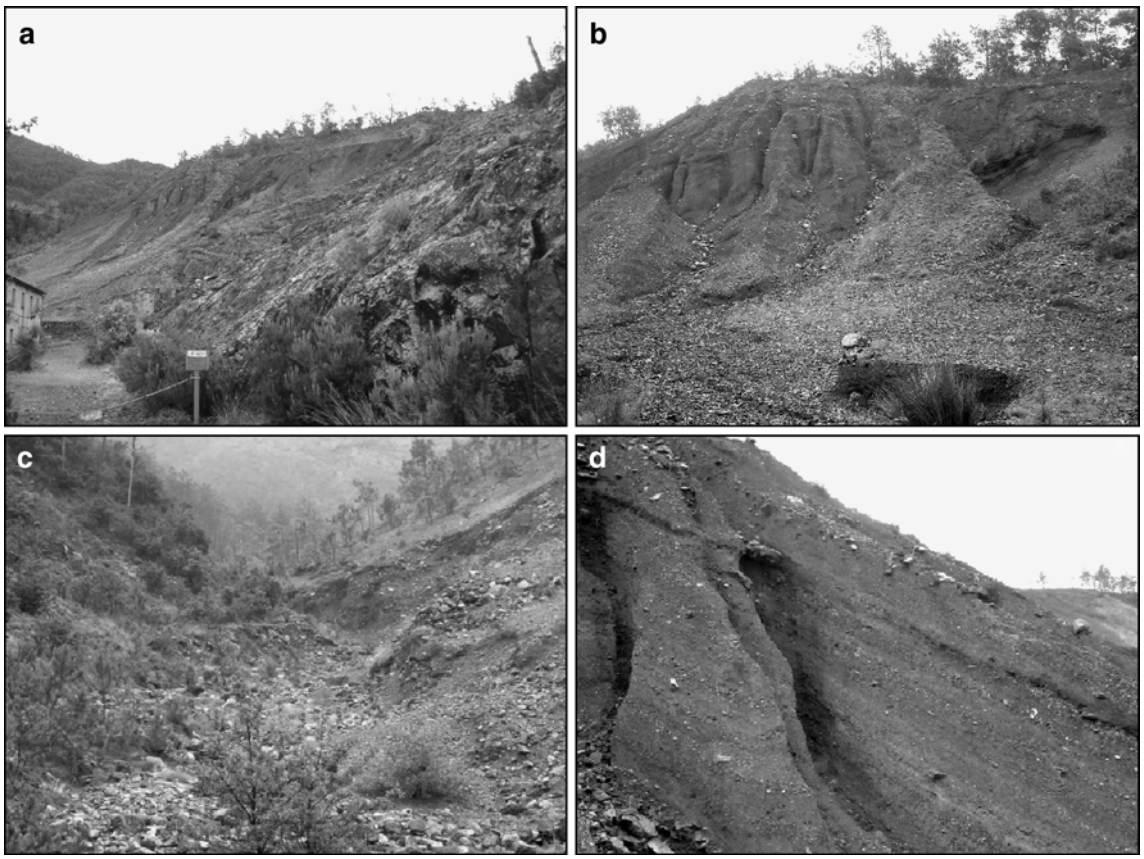

Fig. 2 Different view of the waste-rock dump studied. **a** View of the dump from NW to SE, **b** upper part of the dump, **c** basal part of the dump adjacent to Rio Boeno, **d** centimetric layering on a vertical section of the dump outcropping on the wall of an eroded canyon

surface of the dump and, where substantial enrichments of sulphides are present, these rinds evolve up to dark-brown hardpan.

Sampling and analytical methods

Sampling

Within the waste-rock dump, we defined a rectangular sampling area that covered the entire core of the dump (Fig. 1). This area was further divided into square cells to form a sampling grid where 21 composite samples (about 2 kg) were collected (Fig. 1) by sampling the first 50 cm from the surface with a shovel. We performed the sampling so that all particles in the composite samples had an equal chance of selection. We chose to sample the upper 50 cm of each site because of the ease of collection and because the surficial material would most probably be the most reactive due to having the highest interaction with the weathering agents. Moreover, the physical erosion by rain-wash and local landslides continuously expose new surfaces enabling higher chemical reactivity to occur.

The 21 samples were split into two identical portions for the mineralogical and geochemical analyses performed at the Dipartimento per lo Studio del Territorio e delle sue Risorse (Genova University) and Dipartimento di Scienze della Terra "A. Desio" (Milano University), respectively.

Analytical methods

The particle size distribution was obtained by wet sieving (from >64 to 0.063 mm) and sedigraphy (from <0.063 to 0.0005 mm) following the standard 1/2 phi Krumbein (1934) size classes.

The mineralogy and the petrography of the samples were studied using several techniques, which included optical microscopy (stereoscopic, reflected-light, and transmitted-light microscopy), scanning electron microscopy (SEM) and microanalysis (EDS), and X-ray powder diffraction (XRPD).

The 0.355–0.125 mm fraction was embedded in epoxy resin and then prepared for standard polished thin sections that were then analysed by optical and electron microscopes. The modal abundance was estimated by point

counting, based on 500 counts per section, using a combined transmitted-/reflected-light microscope.

On the same thin sections, selected points were analysed for the mineral chemistry using a Philips SEM 515 electron microscope, equipped with an EDS spectrometer at 15 kV accelerating voltage, 2.15 nA beam current and 10–25 μm beam diameter. Calibration was performed with a set of synthetic and natural standards including pargasite and K-augite (Si, Al, Na, Mg, K, and Ca), ilmenite (Ti and Mn), chromite (Cr), apatite (P), barite (S), hematite and fayalite (Fe), heazlewoodite (Ni), chalcopyrite (Cu), and metals (Cu, Co, Zn, Pb, and Sb).

The XRPD analyses were carried out, on the 0.063–0.016 mm fractions, using a Philips 3710 diffractometer equipped with a Co-anode (CoKα-radiation, current 20 mA, voltage 40 kV) and interfaced with PC-ADP software for data acquisition and processing. Due to the poor crystallinity of the Fe-oxides and Fe-oxyhydroxides, the data were collected over a total acquisition time of about 15 h to improve the peak-to-noise ratio. XRD patterns were obtained in the range 5°–120° 2θ with a step size of 0.030° 2θ, and counting time of 5.5 s per step.

For the geochemical analyses, the fraction ≤2 mm was ground in an agate mill to a fine powder. The major and minor elements (Cr, Cu, Ni, and V), and S_{tot} for each sample were determined by XRF analysis on powder discs using an automated Philips PW 1400 spectrometer. Given the geological features of the samples, the XRF calibration straight line was built using basic and ultrabasic standard rocks. Trace element (Cd, Co, and Zn) concentrations were determined by ICP-AES (Jobin–Yvon JY24) on solutions obtained by acid digestion (0.25 g powder leached with 6 ml 30% HCl Suprapure and 2 ml 65% HNO_3 Suprapure) in a closed microwave oven (Milestone 1200 Mega).

The AMD evaluation of each sample was based on the AMIRA procedure (IWRI and EGI 2002), which is a revision of the Sobek et al. (1978) procedure, that allows the evaluation of the maximum potential acidity (MPA) and the acid neutralising capacity (ANC), both expressed as kg H_2SO_4/t. The ANC was experimentally determined by titration preceded by a "fizz test" as described by Sobek et al. (1978).

Ther major element concentrations, heavy-metal contents, and AMD values were finally processed by means of statistical and geostatistical methods. A semi-variogram analysis was performed to measure the spatial variability of several variables and provided some input parameters for the spatial interpolation of kriging (Krige 1951; Matheron 1963; Webster and Oliver 2001). The natural neighbour gridding method was used to represent the areal distribution of the heavy metals when a spatial relation was not assessed with the semi-variogram analysis. This choice was supported by negative concentration areas, which had no physical meaning, due to kriging interpolation without outlier removal.

The last part of this work was aimed at calculating the persistence of the AMD processes that could be estimated from common data, such as yearly rainfall, mining water pH and acid production or the neutralising potential of the terrains (Servida et al. 2009). These few input data make it possible to determine the potential persistence in time of the processes in years. Even if this number could be refined, the order of magnitude is only useful for classifying the persistence of the processes in three classes: low (<10 years), middle (<100 years) and high (>100 years).

Mineralogy

Mineralogy of the dumped material

All samples were well sorted and they could be classified as sandy–gravely sediments with the exception of five samples that fell into the gravel class and into the muddy gravel class (Folk 1954, 1974). The silt and clay fractions (<0.05 mm) varied from 5 to 26% and were directly proportional to the modal abundance of the authigenic secondary minerals, as demonstrated by the XRPD patterns.

The waste-rock dumps were mineralogically characterised by extremely heterogeneous materials because they comprised minerals constituting the gangue and the host rocks, ore minerals with different degrees of alteration, and authigenic secondary phases that directly formed in situ or allocthonously accumulated within the dump. To define the mineralogy of these materials qualitatively and quantitatively, it is thus necessary not only to distinguish the different mineral species, but also to classify them according to their role in the AMD processes. Following the Jambor and Owens (1993) scheme, we distinguished: (1) primary minerals (comprising ore- and gangue-mineral assemblages) and (2) secondary minerals (comprising all species that directly formed within the dump as alteration products of primary phases). To estimate the modal abundance of the different minerals, the following mineral classes were determined: (1) primary sulphides, (2) primary silicates, (3) primary carbonates, (4) secondary Fe-oxides and Fe-oxyhydroxides, and (5) secondary sulphates. During the counting, each grain was univocally assigned to one specific class when more than 50% of the surface of the grain belonged to that class.

The sulphide ore minerals were represented by pyrite, chalcopyrite, sphalerite, and pyrrhotite, in decreasing order of abundance; other sulphides (such as covellite, chalcocite, and pentlandite) and native elements (Au, Ag, and Cu) were present only as very minor to trace constituents. On the whole, they varied from 0.7 to 40% (median 4.5%;

Table 1) of the waste materials. The lowest and highest contents were anomalous values because they represented sample sites characterised by almost completely inert materials (derived from local open-pit excavations in serpentinites) and highly enriched sulphide materials (derived from handpicking enrichment operations), respectively.

The degree of alteration of the sulphides was quite variable from site to site. It was evaluated following the "sulphide alteration index" (SAI) of Blowes and Jambor (1990) which distinguishes the different alterations through a numerical scale from 10 to 0, on the basis of the relative reactivity of the sulphide species and their degree and style of alteration. In the studied samples, pyrrhotite was never present as completely unaltered crystals, whereas pyrite was found either as completely unaltered idiomorphic grains (Fig. 3a), as partially altered crystals (Fig. 3b, c), and as completely pseudomorphically replaced crystals (Fig. 3d). Chalcopyrite and sphalerite were the best-preserved sulphides and they were usually unaltered or weakly altered along rims and fractures, where they were characterised by narrow alteration rims and oxidation haloes. On the basis of this evidence, the samples studied fell into the classes between 8 and 6 on the SAI (Blowes and Jambor 1990).

The observed relative reactivity of the different sulphides agreed well with the reactivity sequences observed by several authors (Jambor 1994 and references therein), with sphalerite < chalcopyrite < pyrite < pyrrhotite. Nevertheless, several exceptions were observed due to other concomitant factors that influence sulphides weathering such as the habitus and size, the degree of fracturing, and the armouring effect of insoluble secondary mineral coatings on sulphide surfaces. As a matter of fact, despite its high reactivity in an oxidising environment, millimetric idiomorph pyrite crystals were often well preserved or slightly altered, even in samples characterised by a very high degree of alteration, whereas micro- and cryptocrystalline pyrite assemblages were always completely oxidised and replaced by Fe-oxyhydroxides.

Gangue and host-rock minerals varied from 28.9 to 84.9% (median 53.2%; Table 1) of the waste materials and they reflected the two main lithotypes that host the Libiola ore deposit (i.e. pillow and brecciated basalts and serpentinites). The most abundant minerals were serpentine (lizardite and chrysotile), Ca-plagioclase, magnetite, chlorite, clinopyroxene (augite), clay minerals, albite, and quartz, in decreasing order of abundance. Minor amounts of Cr-bearing spinels, Fe-epidote, ilmenite, and zeolites were present in all samples, whereas primary carbonates (calcite, aragonite, and dolomite) were generally only found as trace amounts. The silicates were unaltered or only partially weathered and their degree of alteration was mainly dependent on the mineral species, but also on the grain size and texture and the sulphide content of the samples. In fact, during sulphide oxidation, the local formation of corrosive acids significantly enhanced silicate alteration. Generally, the following relative weathering rates (in order of decreasing resistance) were recognised: serpentine > albite > chlorite > clinopyroxene > Ca-plagioclase > magnetite.

It is worth noting that, although nearly all of the aluminosilicates were only partially to weakly weathered, the great abundance of these minerals found in all the samples explained the very high release of Al and Si into the circulating solutions, as demonstrated by several tests performed on the Libiola ASW (Dinelli et al. 1999; Dinelli and Tateo 2002; Marini et al. 2003; Accornero et al. 2005). Moreover, most of the non-chalcophile metals that were present in significant concentrations within these waters (such as Cr and V) were presumably derived from chromite, spinels, and other ultramafic and mafic minerals.

The secondary minerals were mainly Fe-oxyhydroxides (goethite and minor lepidocrocite) and Fe-oxides (hematite) that represented 13.8–69.3% (median 43.9%; Table 1) of the total constituents. The SEM and XRPD analyses performed on selected samples revealed that these minerals were always present as intimate mixtures of micrometric and submicrometric crystals. On the basis of the main mineral species, two different types of mixtures were distinguished: hematite-rich mixtures (corresponding to red and reddish-brown aggregates) and goethite-rich mixtures (corresponding to yellow and ochreous aggregates). Minor to trace amounts of lepidocrocite were sometimes present in each mixture.

Table 1 Statistical summary of modal abundance (%) of primary and secondary minerals obtained from point counting

	Gangue minerals	Primary sulphides	Sec. minerals (Gt-rich)	Sec. minerals (Hm-rich)	Other minerals	Gt-rich + Hm-rich
Mean	49.73	8.04	27.43	14.45	0.35	41.88
Median	53.20	4.50	29.44	11.55	0.00	43.94
Range	28.95–84.84	0.7–40	10.2–57.7	0.3–40.3	0–1.2	13.8–69.3
SD	19.49	9.57	13.34	11.42	1.11	14.34

Gt-rich goethite-rich secondary minerals, *Hm-rich* hematite-rich secondary minerals, *SD* standard deviation

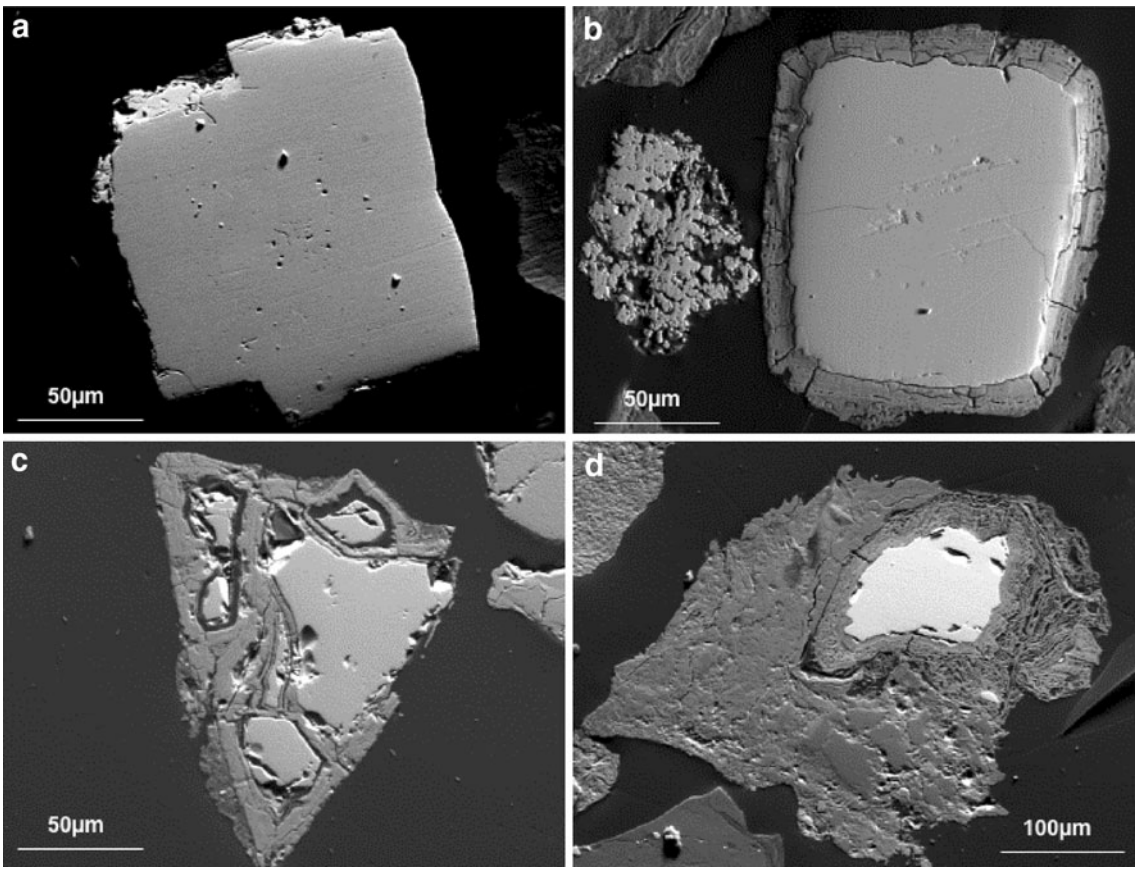

Fig. 3 Style and degree of alteration of sulphide crystals. **a** Unaltered idiomorphic pyrite crystal, **b** idiomorphic pyrite crystal partially replaced by Fe-oxyhydroxides along outer rim, **c** pyrite crystal partially replaced along intergrain fractures, **d** pyrite crystal almost completely replaced by Fe-oxyhydroxides

These secondary minerals could have been precipitated from acid solutions (filling voids, intergranular spaces, intraclast fractures, and porosity) or pseudomorphically replaced the primary sulphides and, to a minor extent, the gangue minerals. The other secondary minerals such as gypsum, malachite, azurite, and native copper were present in minor to trace amounts (Table 1). Soluble hydrous sulphates (such as gypsum, melanterite, epsomite, bieberite, and siderotil) were only common in the waste dump in dry periods. During the sampling performed for this study, they were only observed on the surface of the sampling sites. Nevertheless, during previous surveys (see for example Marescotti et al. 2008) they were commonly present as surficial ephemeral blooms. As demonstrated by Plumlee (1999), these minerals are of environmental concern because they temporarily store acid and metals in the solid phases, but during wet periods their dissolution can result in potentially acidic fluxes into the ground and surface waters.

Finally, clay minerals (mainly montmorillonite and other smectite group minerals) were generally widespread, although only as minor constituents. Nevertheless, it is still not clear if they originated in AMD processes or from geological processes not directly related to sulphide weathering.

Mineral chemistry

The pyrite generally contained significant amounts of copper (range 0.09–2.50 wt%; Table 2), nickel (range 0.10–1.71 wt%; Table 2), and cobalt (range 0.10–0.75 wt%; Table 2). As demonstrated by Zaccarini and Garuti (2008), the Co and Ni contents in pyrite are strongly dependent on host rocks with an average Co/Ni ratio varying from 0.53, in serpentinite-hosted sulphide ores, to 2.87 in basalt-hosted deposits. Zinc (range 0–0.50 wt%; Table 2) and arsenic (range 0–0.40 wt%; Table 2) varied greatly from grain to grain without any systematic correlation with the host rocks or textural and structural features. Anomalous high Zn contents (>1 wt%) could be related to the presence of cryptocrystalline inclusions of sphalerite in the pyrite crystals.

With the exception of Zn (range 0.25–0.80 wt%; Table 2), the chalcopyrite generally contained lower

Table 2 Statistical summary of mineral chemistry (wt%) of pyrite and chalcopirite

	Fe	Cu	Ni	Co	Zn	As	S
Pyrite							
Mean	46.08	0.58	0.68	0.38	0.28	0.25	52.42
Median	45.83	0.38	0.78	0.57	0.18	0.28	52.48
Range	45.67–46.57	0.09–2.50	0.10–1.71	0.10–0.75	0-0.50	0–0.40	52.09–52.94
SD	0.44	0.94	0.69	0.24	0.27	0.13	0.35
Chalcopyrite							
Mean	30.63	34.41	0.19	b.d.l.	0.52	b.d.l.	34.57
Median	30.60	34.41	0.10	b.d.l.	0.38	b.d.l.	34.63
Range	30.49-30.82	34.28–34.53	0.10–0.38	b.d.l.	0.25–0.80	b.d.l.	34.20–34.90
SD	0.13	0.10	0.16	b.d.l.	0.22	b.d.l.	0.28

SD standard deviation, *b.d.l.* below detection limits

amounts of minor and trace elements than the pyrite. The few analyses performed on sphalerite (9 analyses) and covellite (3 analyses) constantly demonstrated high contents of Cu (up to 0.60 wt%) and Ni (up to 1.50 wt%) in the sphalerite and Co (up to 0.27 wt%) and Zn (up to 0.20 wt%) in covellite.

It was never possible to obtain data on the mineral chemistry of the Fe-oxide and Fe-oxyhydroxide single crystals from the samples studied because, as stated before, they occurred as mixtures of crystals with a size below the analytical resolution of SEM. Therefore, we analysed Fe-oxide and Fe-oxyhydroxide mixtures by subdividing the goethite-rich and the hematite-rich mixtures on the basis of their mode of occurrences, i.e. fractures and voids fillings and pseudomorphic replacement of primary sulphides.

Goethite-rich and hematite-rich mixtures occurring as voids and fractures fillings showed similar low concentrations of alkaline and alkaline-earth elements and similar high Cu and S contents (Table 3). Significant concentrations of Si, Al, and Cr were present in both types, but the hematite-rich mixtures always had higher concentrations of these elements (Table 3). Finally, the goethite-rich mixtures were remarkably enriched with Ni (range 0.19–1.03 wt%; Table 3) and Co (range 0.19–0.95 wt%; Table 3), whereas the hematite-rich mixtures showed the highest Zn contents (range 0.19–0.44 wt%; Table 3).

It is worth noting that significant differences were revealed in the Fe-oxide and Fe-oxyhydroxide mixtures occurring as pseudomorphic replacements of primary sulphides. These mixtures invariably had the highest S contents (range 3.1–4.52 wt%; Table 3), the lowest amounts of Si and Al, and negligible amount of alkaline and alkaline-earth elements (Table 3).

Table 3 Statistical summary of mineral chemistry (wt%) of secondary Fe-oxide and Fe-oxyhydroxide mixtures

	Si	Al	Fe	Mg	Ca	Na	K	Cr	Co	Ni	Cu	Zn	S
Hematite-rich mixtures (fillings)													
Mean	7.00	2.31	64.63	0.32	0.25	0.06	0.09	0.77	0.07	0.11	1.35	0.31	0.32
Median	6.91	2.29	64.77	0.32	0.26	0.05	0.08	0.76	0.07	0.11	1.39	0.30	0.29
Range	6.08–8.09	2.20–2.48	63.44–65.42	0.19–0.44	0.19–0.29	0.05–0.08	0.06–0.12	0.66–0.89	0.05–0.09	0.09–0.15	1.14–1.48	0.19–0.44	0.24–0.46
SD	1.03	0.13	0.94	0.18	0.04	0.02	0.03	0.10	0.03	0.03	0.15	0.12	0.10
Goethite-rich mixtures (fillings)													
Mean	4.30	1.34	56.16	0.15	0.15	0.27	0.07	0.22	0.44	0.86	1.95	b.d.l.	0.37
Median	4.21	1.36	56.69	0.15	0.15	b.d.l.	0.06	0.23	0.45	0.75	2.09	b.d.l.	0.41
Range	2.42–6.34	0.77–1.88	53.21–58.05	0.09–0.21	0.10–0.19	b.d.l.	0.06–0.10	0.08–0.36	0.19–0.95	0.19–1.03	1.24–1.37	b.d.l.	0.14–0.53
SD	1.67	0.47	2.17	0.08	0.05	b.d.l.	0.02	0.13	0.34	0.14	0.52	b.d.l.	0.18
Fe-oxide and Fe-oxyhydroxide mixtures (pseudomorphic)													
Mean	0.79	0.28	56.13	0.07	0.08	b.d.l.	0.08	0.14	0.32	0.25	1.54	0.29	4.04
Median	0.80	0.29	55.64	0.07	0.09	b.d.l.	0.08	0.15	0.32	0.24	1.48	0.24	4.26
Range	0.65–0.89	0.21–0.33	55.09–58.17	0.05–0.09	0.07–0.09	b.d.l.	0.07–0.09	0.09–0.17	0.21–0.41	0.19–0.31	1.31–1.38	0.09–0.59	3.12–4.52
SD	0.10	0.05	1.44	0.03	0.01	b.d.l.	0.01	0.04	0.09	0.06	0.26	0.24	0.62

SD standard deviation, *b.d.l.* below detection limits

On the whole, these minerochemical features confirm the ability of secondary Fe-oxides and Fe-oxyhydroxides to incorporate remarkable amounts of metals and other elements dissolved by the acid solutions through isomorphous substitutions or absorption and coprecipitation mechanisms. Moreover, it was evident that the minerochemical features are controlled by the mineral species that are present within the secondary assemblages (i.e. hematite and goethite) but also by their mode of occurrence. As an example, the remarkably high S content of the pseudomorphosis was clearly related to the local sulphur enrichments released into the circulating solutions during sulphide oxidation.

Finally, in all the analysed samples and, in particular, in the pseudomorphic replacements, a partial contribution of residual cryptocrystalline primary minerals, intimately mixed with the newly formed secondary phases, cannot be excluded.

Geochemistry

Bulk chemistry of the dumped materials

The analyses and the statistical summaries of the elemental bulk composition of the dumped materials are given in Table 4. The geochemical signatures of the waste-rock samples agreed well with the qualitative and quantitative results of the mineralogical analyses. Fe, Si, Mg, and Al were always the main constituents, reflecting the nature of the main lithotypes (serpentinites and basalts) deposited in the dump and the presence of high amount of secondary Fe-rich mineral phases. The sulphur showed notable variations (from 0.01 to 5.71 wt%; Table 4) due to the high variability of the sulphide minerals (particularly pyrite) within the dump. Moreover, the almost complete absence of sulphates and the low S contents in the other secondary minerals (Table 4) suggested that most of the sulphur released during sulphide alteration had been removed from the system.

The other metals (such as Ti, Mn, Co, Ni, V, Cr, Cu, Zn, and Cd) that generally had a high concentration and a notable variability could not be clearly correlated with the mineralogical composition of the samples. In fact, these elements could be contained in both the unaltered primary minerals and the secondary Fe-oxides and Fe-oxyhydroxides (Table 3).

AMD evaluation

According to the AMIRA procedure (IWRI and EGI 2002), the AMD was evaluated through the following two parameters: MPA and ANC.

Table 4 Statistical summary of bulk elemental composition of waste-rock samples

	SiO_2 (wt%)	Al_2O_3 (wt%)	Fe_2O_3 (wt%)	MgO (wt%)	CaO (wt%)	TiO_2 (wt%)	MnO (wt%)	Na_2O (wt%)	P_2O_5 (wt%)	Cr (ppm)	Co (ppm)	V (ppm)	Cu (ppm)	Zn (ppm)	Ni (ppm)	Cd (ppm)	S (wt%)
Min	28.94	1.15	18.26	2.32	0.13	0.17	0.01	0.03	0.07	215	31	112	160	33	93	1	0.01
25 percentile	33.84	7.32	27.85	7.75	0.65	1.33	0.01	0.07	0.13	541	59	223	1,258	130	224	9	0.04
Median	36.60	8.24	38.98	10.82	0.72	1.78	0.04	0.16	0.19	846	78	302	1,887	196	435	13	0.66
75 percentile	40.51	10.34	42.16	21.63	1.12	2.27	0.11	0.45	0.25	1,259	104	365	3,022	317	1,063	17	1.07
Max	46.12	18.08	51.33	26.73	1.97	3.08	0.35	0.69	0.29	2,524	408	541	13,347	1,126	3,579	23	5.71
Mean	37.12	9.05	35.98	14.39	0.88	1.86	0.07	0.26	0.18	1,019	102	309	1,885	277	885	14	0.75
SD	4.62	3.38	9.79	7.25	0.51	0.71	0.09	0.22	0.07	621.59	83.79	106.72	1,044.89	245.50	1,038.33	5.19	0.80

SD standard deviation

MPA is an estimate of the amount of acid that the sample can release by complete oxidation of sulphides. The evaluation of MPA by the AMIRA standard procedure is based on the conservative assumption that all S is present as pyrite. This simplification may overestimate the AMD as other sulphides with higher Me/S ratios have lower acid generation potential than pyrite. Moreover, such an overestimation can give unrealistic results where high percentages of S are present as non-acid-generating phases (i.e. sulphates).

ANC is an estimate of the capacity of the samples to neutralise the acidity produced during AMD processes. When a negative ANC value was obtained, it was reported as 0.00, indicating the sample was incapable of neutralisation.

The difference between MPA and ANC is referred to as the net acid producing potential (NAPP). NAPP is a theoretical value commonly used to indicate whether waste material has potential to generate AMD. When NAPP is negative, it indicates that a sample may have sufficient ANC to prevent acid generation. Conversely, if the NAPP is positive the material may be acid generating.

The results (Table 5; Fig. 4a) showed that in the waste-rock dump studied, the potential for AMD generation was widespread with MPA values ranging from 0.31 to 148.72 kg H_2SO_4/t. The NAPP coincided with the MPA values because the ANC of all the samples was negative with the exception of sample 21. Since mineralogical investigations have shown that sulphate occurrence is negligible, these AMD values were reliable. So, it was not necessary to analyse samples for S-sulphate to obtain the MPA value calculated starting from S-sulphur. This was also confirmed by the similar trend that we obtained by plotting the NAPP versus the total S (obtained by bulk chemistry analyses; Fig. 4a) and versus the sulphide modal abundance (obtained by point counting; Fig. 4b).

Following the Soregaroli and Lawrence (1997) classification (Fig. 4a), eight samples fell in "field I", which indicated that the AMD was possible but did not persist over time due to the low S content. Twelve samples fell in "field II", indicating that the AMD was possible and persisted over time due to the high S content. Only one sample fell in "field III" (sample 21) which indicated that the AMD was impossible; this sample was representative of an area where the dumped materials were almost exclusively represented by poorly mineralised serpentinite- and basalt-rich waste rock derived from open-pit excavations.

Geostatistical analysis

Due to the great heterogeneity of the mineralogical, geochemical and AMD data, a spatial analysis was performed to estimate the value of the different variables in the entire mine dump area. The semivariogram results showed that all the variables, with the exception of Cu, had a spatial

Table 5 AMD calculation results

Sample	Total S (wt%)	MPA (kg H_2SO_4/t)	ANC (kg H_2SO_4/t)	NAPP (kg H_2SO_4/t)
1	0.04	1.22	−32.07	1.22
2	0.01	0.31	−30.26	0.31
3	0.01	0.31	−28.93	0.31
4	0.66	20.20	−47.22	20.20
5	0.02	0.61	−31.55	0.61
6	0.73	22.34	−42.45	22.34
7	2.50	76.50	−35.21	76.50
8	2.22	67.93	−40.03	67.93
9	2.11	64.57	−41.67	64.57
10	0.01	0.31	−32.71	0.31
11	1.34	41.00	−37.14	41.00
12	0.98	29.99	−36.68	29.99
13	1.07	32.74	−49.67	32.74
14	0.50	15.30	−39.18	15.30
15	0.99	30.29	−39.04	30.29
16	0.13	3.98	−31.83	3.98
17	0.01	0.31	−30.72	0.31
18	0.74	22.64	−42.85	22.64
19	0.22	6.73	−34.16	6.73
20	5.71	148.72	−37.00	148.72
21	0.50	15.30	83.92	−68.62

When a negative value of ANC is obtained it indicates the sample is incapable of neutralisation. Therefore, it is reported as 0.00 in the formula for the calculation of the NAPP. Samples 20 and 21 from Marescotti et al. (2008)

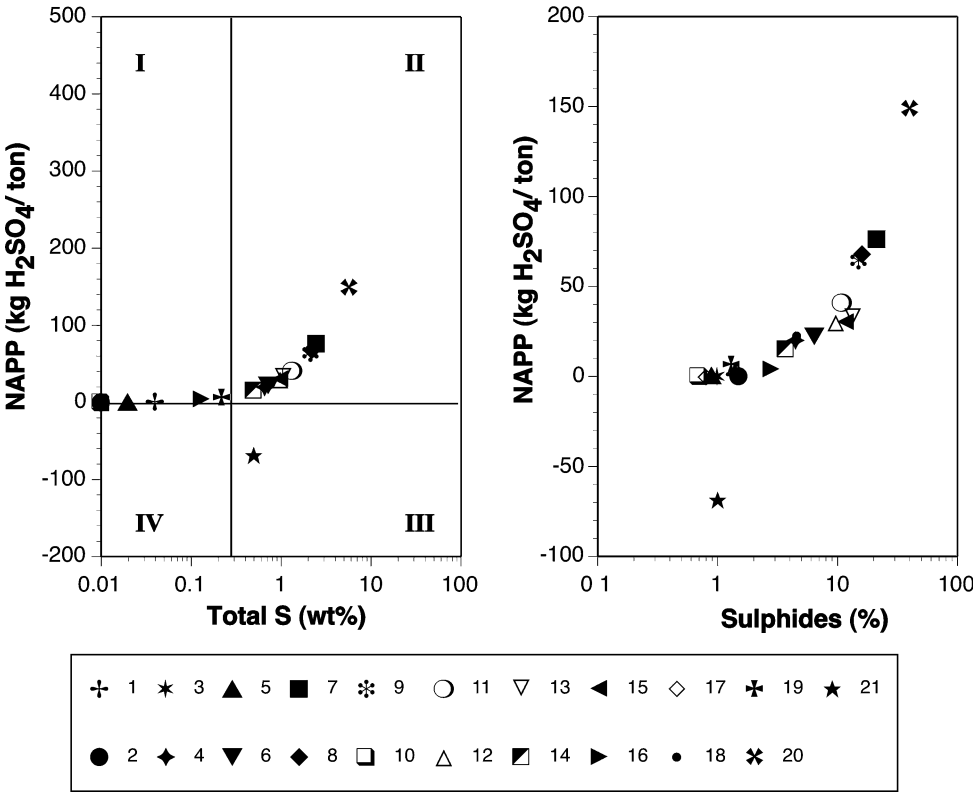

Fig. 4 **a** NAPP values vs. total S content (from Soregaroli and Lawrence 1997). *Field I* AMD possible but non-persisting over time. *Field II* AMD possible and persisting over time. *Fields III* and *IV* AMD impossible. **b** NAPP value versus sulphides modal abundance as determined by point counting. Samples 20 and 21 from Marescotti et al. (2008)

relationship. After this test, a contour map was drawn for each variable with kriging interpolation, whereas the contour map of Cu was drawn with a natural neighbour interpolation. Contour maps (Fig. 5) make it possible to display the different variable distributions of the most significant chemical elements and mineral species and to point out direct and inverse correlations, as well as to define areas with peculiar characteristics. On the basis of the contour-map analysis, the studied mine dump could be subdivided into three main zones:

1. The first zone (Fig. 5), located in the NW sector of the dump, was characterised by a narrow area with high concentrations of total sulphur (directly proportional to the NAPP values), Cu, Fe_2O_{3tot}, primary sulphides, and local enrichment with goethite (Fig. 5).
   These results agreed well with the historical documents (Marescotti and Carbone 2003 and references therein) and with the results of field observations. In fact, this area historically represented the lowest level of the dump, where the extracted mineralisations were placed and preliminarily treated by means of hand picking and manual selection. The non-economic mineralisations were left in place and contained a high percentage of pyrite and minor chalcopyrite minerals. Field observations make it possible to recognise the presence of thick ochreous crusts that locally evolved up to centimetric dark reddish hardpans in most of the zone. Moreover, numerous partially unaltered mineralised clasts were easily observable either on the surface of the dump or in the sampled vertical sections.
2. The second zone (Fig. 5), positioned in the SW sector of the dump, corresponded to a topographical plain close to three mine adits and one of the biggest open pits of the mine area. This zone was characterised by the highest Fe_2O_{3tot} and goethite concentrations with intermediate total sulphur (NAPP) values. The chemical and mineralogical features of this zone could be related to the diffuse presence of non-economic sulphides deposited in situ during exploitation. As a matter of fact, most of the outcropping rocks in the adjoining area was characterised by the diffuse presence of pyrite-rich stockwork mineralisations. The lower NAPP values than the NW zone could be related either to the lower concentration of sulphides in the dumped rocks or a general more advanced degree of alteration. This is also confirmed by the higher concentrations of secondary minerals (goethite and minor hematite).
3. The third zone (Fig. 5), located in the N and NE sectors of the dump, was characterised by the highest concentration of MgO, Cr_2O_3, Ni, and primary silicate minerals. These features could be correlated to the diffuse presence of ophiolitic clasts (serpentinites and

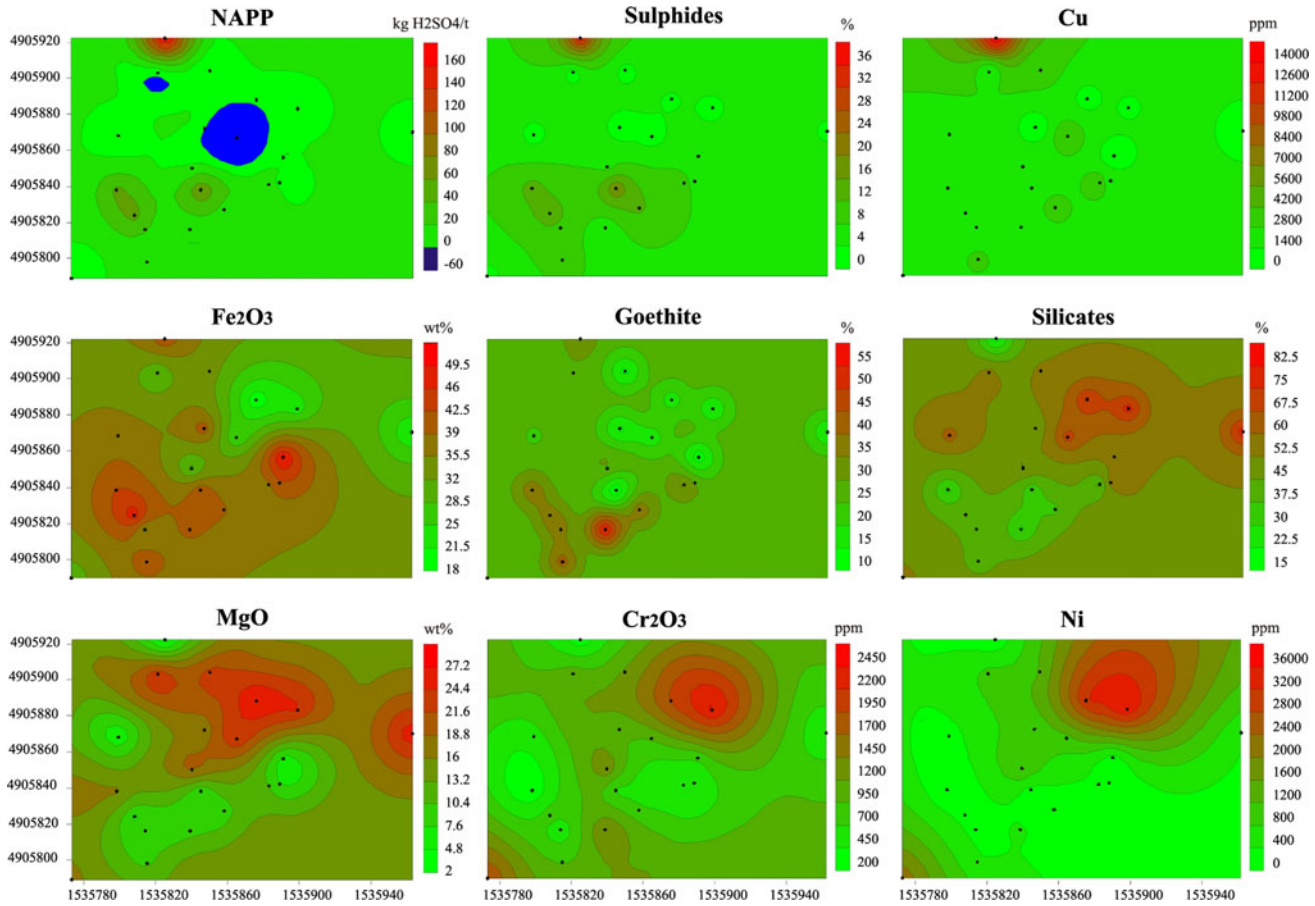

Fig. 5 Contour maps of selected elements (Fe_2O_3, MgO, Cr_2O_3, Cu, and Ni), NAPP, and minerals (sulphides, goethite, and silicates)

basalts), mainly derived from the upper open-pit excavations and piled up mainly in this sector of the dump.

Other than the above-mentioned features, it is important to outline that the Cu contents were generally high in the entire mine dump and seemed to be independent of the other element concentrations. The Cu distribution was homogeneous with the exception of zone 1 described above. These features could be related to the scattered distribution of Cu-rich pyrite and chalcopyrite remnants throughout the dump due to the extensive mining activity that affected this site over more than a century.

Persistence of the AMD processes

Using the monthly temperatures provided by Eurometeo (1999), the evapotranspiration rates were calculated for the study area according to Thornthwaite (1948). This parameter affects 54% of the water balance, on average, and its highest values are reached from April to September, when evapotranspiration is 100% of precipitation, whereas the lowest are in December (16%). The remaining meteoric waters could flow over the surface or infiltrate the ground. Surface flow was evaluated at 29% and infiltration at 17% of the water balance with the Soil Conservation Service Curve Number (USDA-SCS 1972) method.

Assuming that 802.0 mm/year of rain falls on the Libiola catchment area (Provincia di Genova 2002), 430.6 mm/year were lost through evapotranspiration, 235.1 mm/year flowed over the surface and 136.1 mm/year infiltrated the ground. Considering that the Libiola catchment area covers 4.0×10^4 m^2 and that only 3.6×10^4 m^2 are upstream from the NAPP > 0 area, it is possible to calculate that 9.4×10^3 m^3/year of meteoric water are available for the AMD generation processes.

The pH value of the rain water was assumed to be 5.66, but the calculations are not sensitive to such a value.

The average surface water pH value in the area studied ranged from 3.44 to 4.89 (Carbone 2008). The lowest pH value implied an H^+ concentration of 0.36 mg/l, whereas the highest pH value implied an H^+ concentration of 0.01 mg/l. From 6 to 167 kg H_2SO_4/year would be needed to keep these pH values constant for all the rain water falling on the studied area. Since the average NAPP value of earth materials is 22.95 kg H_2SO_4/t, and assuming a

reactive thickness of 0.50 m (as this is the earth material that mostly interacts with atmospheric agents and is the depth to which the earth material samples were collected) and an average density of 2.50 g/cm^3, these earth materials could produce as much as 1.03×10^6 kg of H_2SO_4. So, if the environmental and climatic conditions do not change, dividing the total amount of H_2SO_4 equivalent (that can be released) by the total amount of H_2SO_4 equivalent (necessary to maintain the present pH values of the waters) the present conditions could endure from 6.17×10^3 to 1.74×10^5 years.

Discussion

- The mineralogical and geochemical data highlighted that the waste-rock dump studied is still affected by significant AMD processes that can produce huge amounts of acids for a long period to come. This is also indirectly confirmed by the acidity of the waters of the adjacent stream (Rio Boeno) that collects most of the contaminated solutions leaching out from the dump. Furthermore, as revealed by a previous work (Marescotti et al. 2008), the waste materials deposited in this dump exceed commercial and industrial concentration limit for most heavy and transition metals, according to Italian law (D.M. 471/1999; D.Lgs 152/2006).
  This scenario is due to several concomitant factors such as: (a) the high content and the widespread distribution of reactive sulphide mineralisations, (b) the almost complete lack of mineral species or lithotypes (carbonates and/or calcareous rocks) able to neutralise or minimise the acidity, (c) the high permeability of the dump due to the coarseness of the dumped materials and the absence of a constant water-saturated zone, and (d) the widespread erosive processes affecting the whole dump that continuously expose new surfaces to supergenic oxidation.
- The environmental situation is exacerbated by the release, to the circulating solutions, of high amounts of potentially toxic metals during weathering of sulphide mineralisations (Fe, Cu, Zn, etc.) and host rocks (Cr, Ni, V, etc.).
- Another major effect of the ongoing AMD processes is the production of huge amounts of secondary minerals from the circulating solutions. They precipitate not only in the adjoining stream beds but also on and within the dump where they form crusts that cap the surface or fill voids and interstices between clasts. Once formed, these minerals are relatively insoluble in supergenic environments and thus they play a key role in the physical and chemical properties of the waste dump. In fact, they progressively decrease the hydraulic conductivity, thus restricting the amount of oxidising water descending through the unsaturated zone. Furthermore, they tend to form concentric rinds around the edge of the sulphide-mineralised clasts, thus determining an effective armouring effect that reduces the rates of sulphide oxidation. Finally, they can store significant amounts of potentially deleterious metals that can be incorporated in the structure as well as adsorbed or coprecipitated (Cornell and Schwertmann 1996 and references therein).
  Nevertheless, recent studies (Carbone et al. 2005a, b) also highlighted that these minerals continuously undergo evolution through dissolution and recrystallization processes; therefore, most of the scavenged toxic metals can be released to solutions during transformation processes induced by variations in the physico-chemical parameters or by ageing. For these reasons, the positive environmental effect related to the precipitation of Fe secondary minerals is not permanent, often contrasting and not easily predictable.
- The waste-rock dump studied was extremely heterogeneous from the mineralogical and geochemical points of view. The significant lateral variations, revealed by the geostastistical analyses, and the vertical heterogeneity, noted in exposed vertical sections, are common and expected features of all mine dumps constructed over long periods of time.
  The Libiola mine dumps were formed in a period of over 50 years during which different techniques of exploitation were used and different lithotypes and economic mineralisations were extracted, through both underground and open-air excavations. The waste materials that were piled up during exploitation comprise both the host rocks and the non-economic mineralisations derived from hand picking, milling, and other treatments. As a consequence, although previous studies (Marescotti and Carbone 2003; Carbone et al. 2005a; Marescotti et al. 2008) indicated that this dump was a highly reactive body capable of producing long-term AMD processes, it was now evident that there is a strong zoning of AMD parameters within the dump.

Conclusions

On the basis of the results obtained it is evident that the knowledge of the spatial mineralogical and geochemical distribution data is of paramount importance for identifying the most critical areas for AMD production within huge open-air waste-rock dumps. These data should, therefore, be considered in the prediction of AMD potential, using

simplified geochemical models, for every plan of remediation. This surficial characterisation of the dump is clearly not extendible to the whole volume of the dump, but it is an important starting point, also for the planning of vertical characterisations through drilling or excavation.

Acknowledgments The authors (P.M., C.C., and G.L.) wish or alternatively the authors (P. Marescotti, C. Carbone, and G. Lucchetti) wish to acknowledge the financial support of MIUR (Italian) Ministero dell'Istruzione, dell'Universita' e della Ricerca (PRIN-COFIN2006): "The role of mineral phases in the mobilisation and storage of contaminant elements within mining sites of eastern Liguria".

References

Abbate E, Bortolotti V, Principi G (1980) Appennine Ophiolites: a peculiar oceanic crust. Ofioliti Spec Iss "Thethian Ophiolites: 1, western area", vol 1, pp 59–96

Accornero M, Marini L, Ottonello G, Vetuschi Zuccolini M (2005) The fate of major constituents and chromium and other trace elements when acid water from the derelict Libiola mine (Italy) and mixed with stream waters. Appl Geochem 20:1368–1390

Blowes DW, Jambor JL (1990) The pore-water geochemistry and the mineralogy of the vadose zone of sulfide tailings, Waite Amulet, Quebec, Canada. Appl Geochem 5:327–346

Carbone C (2008) Cristallochimica e minerogenesi di ossidi e osssiidrossidi di ferro correlati a processi di AMD (Acid Mine Drainage) nell'area mineraria di Libiola (Sestri Levante, GE). Ph.D. Thesis, University of Genova, p 282

Carbone C, Di Benedetto F, Marescotti P, Martinelli A, Sangregorio C, Cipriani C, Lucchetti G, Romanelli M (2005a) Genetic evolution of nanocrystalline Fe-oxides and oxyhydroxides assemblages from the Libiola mine (eastern Liguria, Italy): structural and microstructural investigations. Eur J Miner 17:785–795

Carbone C, Di Benedetto F, Marescotti P, Sangregorio C, Sorace L, Lima N, Romanelli M, Lucchetti G, Cipriani C (2005b) Natural Fe-oxides and -oxyhydroxides nanoparticles: an EPR and SQUID investigation. Miner Petrol 85:19–32

Cornell RM, Schwertmann U (1996) The iron oxides: structure properties, reactions, occurence and uses. VCH Weinheim, USA, p 573

D.Lgs 152/2006—Decreto Legislativo n. 152 del 3 aprile (2006) Norme in materia ambientale. Gazzetta Ufficiale Supplemento ordinario no. 96

D.M. 471/1999—Decreto Ministeriale no. 471 del 25 ottobre (1999) Regolamento recante criteri, procedure e modalità per la messa in sicurezza, la bonifica e il ripristino ambientale dei siti inquinati ai sensi dell'art. 17 del D.Lgs. 22/97 e successive modificazioni e integrazioni. Gazzetta Ufficiale no. 293 del 15 dicembre 1999 Supplemento ordinario 218/L

Dinelli E, Tateo F (2002) Different types of fine-grained sediments associated with acid mine drainage in the Libiola Fe–Cu mine area (Liguria Apennines, Italy). Appl Geochem 17:1081–1092

Dinelli E, Cortecci G, Lucchini F, Fabbri M (1999) REE mobility associated to acid mine drainage: investigation in the Libiola area, northern Italy. GES-5, 16–20 August 1999, Reykjavìc, Iceland

Eurometeo (1995–2008) http://www.eurometeo.com

Folk RL (1954) The distinction between grain size and mineral composition in sedimentary rock nomenclature. J Geol 62:344–359

Folk RL (1974) Petrology of sedimentary rocks. Hemphill Publishing Co., Austin, p 182

Ian Wark Research Institute (IWRI) Environmental Geochemistry International (EGI) (2002) ARD test handbook. AMIRA P387A Project: prediction and kinetic control of acid mine drainage. AMIRA International, Melbourne

Jambor JL (1994) Mineralogy of the sulphide-rich tailings and their oxidation products. In: Jambor JL, Blowes DW (eds) The environmental geochemistry of sulphide mine waste. Mineral Association of Canada Short Course Handbook 22. Mineral Association of Canada, Ottawa

Jambor J L, Owens D R (1993) Mineralogy of tailing impoundment at the former Cu-Ni deposit of Nickel Rim Mines Ltd., eastern edge of the Sudbury structure, Ontario. Division Report CANMET MSL 93-4 (CF), Department Energy Mines Resources, Canada

Krige DG (1951) A statistical approach to some basic mine valuation problems on the Witwatersrand. J Chem Metall Min Soc S Afr 52:119–139

Krumbein WC (1934) Size frequency distributions of sediments. J Sedim Res 4:65–77

Marescotti P, Carbone C (2003) La miniera dismessa di Libiola (Sestri Levante, Liguria Orientale): studio mineralogico sui processi di alterazione di solfuri di Fe e Cu e valutazione del loro impatto ambientale. GEAM 109:45–53

Marescotti P, Carbone C, De Capitani L, Grieco G, Lucchetti G, Servida D (2008) Mineralogical and geochemical characterisation of open pit tailing and waste rock dumps from the Libiola Fe-Cu sulphide mine (Eastern Liguria, Italy). Environ Geol 53:1613–1626

Marini L, Saldi G, Cipolli F, Ottonello G, Vetuschi Zuccolini M (2003) Geochemistry of water discharges from the Libiola mine, Italy. Geochem J 37:199–216

Matheron G (1963) Principles of geostatistics. Econ Geol 58:1246–1266

Plumlee GS (1999) The environmental geology of mineral deposits. In: Plumlee GS, Logsdon MJ (eds) The environmental geochemistry of mineral deposits. Reviews in Econ Geol B 6:71–116

Provincia di Genova (2002) Technical and Normative Document Approved with Legislative Decree 68/02, Piano di bacino, stralcio sul rischio idrogeologico. Torrente Gromolo, pp 133

Servida D, Grieco G, De Capitani L (2009) Geochemical hazard evaluation of sulphide-rich iron mines: The Rio Marina district (Elba Island, Italy). J Geochem Explor 100:75–89

Sobek AA, Schuller WA, Freeman JR, Smith RM (1978) Field and laboratory methods applicable to overburdens and minesoils. U.S. Environmental Protection Agency, EPA-600/2-78-054, Cincinnati, pp 47–50

Soregaroli BA, Lawrence RW (1997) Waste-rock characterisation at Dublin Gulch: a case study. In: Proceedings on the 4th international conference on Acid Rock Drainage. Vancouver, pp 631–645

Thornthwaite CW (1948) An approach toward a rational classification of climate. Geogr Rev 38:55–94

USDA-SCS, U.S. Department of Agriculture-Soil Conservation Service (1972) Estimation of Direct Runoff From Storm Rainfall. In: SCS National Engineering Handbook, Section 4, Hydrology. Chapter 10, U.S. Department of Agriculture, Soil Conservation Service, Washington, D.C., pp 10.1–10.24

Webster R, Oliver MA (2001) Geostatistics for environmental scientists. Wiley, Chichester

Zaccarini F, Garuti G (2008) Mineralogy and chemical composition of VMS deposits of northern Apennine ophiolites, Italy: evidence for the influence of country rock type on ore composition. Miner Petrol 84:61–83